

New Mobility Model for Accurate Modeling of Transconductance in FDSOI MOSFETs

Yen-Kai Lin¹, Student Member, IEEE, Pragya Kushwaha², Juan Pablo Duarte³, Student Member, IEEE, Huan-Lin Chang, Member, IEEE, Harshit Agarwal⁴, Sourabh Khandelwal, Member, IEEE, Angada B. Sachid⁵, Member, IEEE, Michael Harter, Josef Watts⁶, Yogesh Singh Chauhan⁷, Senior Member, IEEE, Sayeef Salahuddin, Senior Member, IEEE, and Chenming Hu, Life Member, IEEE

Abstract—Anomalous transconductance with nonmonotonic back-gate bias dependence observed in the fully depleted silicon-on-insulator (FDSOI) MOSFET with thick front-gate oxide is discussed. It is found that the anomalous transconductance is attributed to the domination of the back-channel charge in the total channel charge. This behavior is modeled with a novel two-mobility model, which separates the mobility of the front and back channels. These two mobilities are physically related by a charge-based weighting function. The proposed model is incorporated into BSIM-IMG and is in good agreement with the experimental and simulated data of FDSOI MOSFETs for various front-gate oxides, body thicknesses, and gate lengths.

Index Terms—BSIM-IMG, fully depleted silicon-on-insulator (FDSOI), gate oxide, image sensor, mobility, transconductance.

I. INTRODUCTION

FULLY depleted silicon-on-insulator (FDSOI) MOSFETs are the promising devices for low static power applications with a good short-channel behavior using the lightly doped body which benefits the carrier mobility and reduces the threshold voltage variation [1], [2]. The threshold voltage of FDSOI MOSFET can be adjusted by the back-gate voltage (V_{BG}) without relying on channel doping concentration control for multiple devices [3], [4]. Furthermore, due to high back-gate bias, an inversion channel may form at the back-side

interface, leading to the distinct characteristics in current and the complicated physics of mobility in FDSOI devices [5]. For example, it is reported that the mobility of front and back channels is different because of remote Coulombic scattering due to charged centers in the polysilicon gate [6]. In addition, the front- and back-interface qualities are different due to the gate-stack. The back-gate bias also affects the carrier's spatial distribution and charge centroid, resulting in a significant deviation from universal mobility curve (UMC). In fact, the definition of effective electric field for UMC is ambiguous for FDSOI devices under the condition of back-side inversion [7], [8]. Due to the complex effects of the back-gate bias on charge and mobility, the transconductance ($g_m = dI_{DS}/dV_{GS}$) of FDSOI MOSFET exhibits significantly different behaviors [9] from bulk MOSFET [10] or FinFET. In this paper, the anomalous transconductance of an FDSOI MOSFET with thick front-gate oxide is explained and modeled. Although FDSOI MOSFET is usually used in low-power circuits [11], in order to fulfill the high-voltage requirement a thick front-gate oxide is adopted [12]. A thick front-gate oxide is also used in image sensor applications with FDSOI MOSFETs [13], [14], where the noise density is reduced by the thick front-gate oxide [15]. In CMOS image sensor architecture design, an accurate transconductance model is required to describe the analog gain in analog signal processor and then output to the analog-to-digital converter [16]. Thus, there is a need to develop a model for FDSOI MOSFETs with thick front-gate oxides. The new mobility model is divided into the front and back components. The final effective mobility uses charges as the weighting factor. The model is validated with the experimental data of FDSOI devices with different front-gate oxides, body thicknesses, and gate lengths.

II. UNDERSTANDING TRANSCONDUCTANCE AND COMPACT MODELING

A. Transconductance Behavior

One of the advantages of the FDSOI MOSFET is the changeable threshold voltage via applying the back-gate bias. If the back-side inversion is absent (only depletion at the back interface), the threshold and thus the transconductance are only shifted by the back-gate bias via capacitive coupling, indicating that only the front mobility is important, as shown

Manuscript received October 29, 2017; accepted December 15, 2017. Date of publication January 3, 2018; date of current version January 22, 2018. This work was supported in part by the Semiconductor Research Corporation under Grant 2671.001 and in part by the Berkeley Device Modeling Center, University of California at Berkeley, Berkeley, CA 94720 USA. The review of this paper was arranged by Editor A. Schenk. (Corresponding author: Yen-Kai Lin.)

Y.-K. Lin, P. Kushwaha, J. P. Duarte, H.-L. Chang, H. Agarwal, A. B. Sachid, S. Salahuddin, and C. Hu are with the BSIM Group, Department of Electrical Engineering and Computer Sciences, University of California at Berkeley, Berkeley, CA 94720 USA (e-mail: ykclin@berkeley.edu).

S. Khandelwal is with the Department of Science and Engineering, Macquarie University, Ryde, NSW 2109, Australia (e-mail: sourabh.khandelwal@mq.edu.au).

M. Harter and J. Watts are with GLOBALFOUNDRIES, Malta, NY 12020 USA.

Y. S. Chauhan is with the Nanolab, Department of Electrical Engineering, IIT Kanpur, Kanpur 208016, India (e-mail: chauhan@iitk.ac.in).

Color versions of one or more of the figures in this paper are available online at <http://ieeexplore.ieee.org>.

Digital Object Identifier 10.1109/TED.2017.2785248

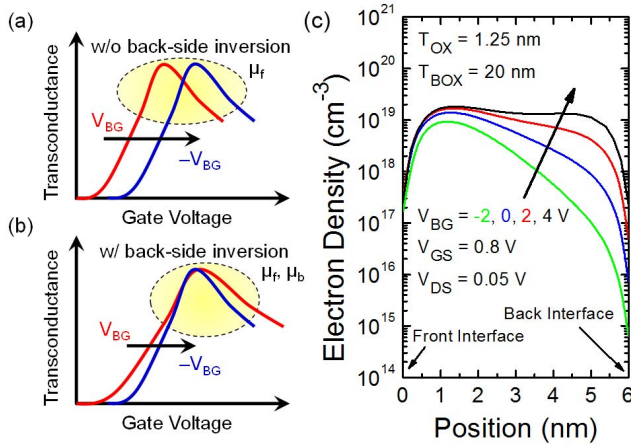


Fig. 1. (a) Typical and (b) anomalous transconductances of the FDSOI nMOSFETs. Due to the back-side inversion, both the front- and back-side mobilities affect the transconductance behavior. (c) TCAD simulated electron density with various V_{BG} .

in Fig. 1(a). In contrast, if there is an inversion at the back interface, the contribution of the back channel is not negligible and the back-side mobility should be considered, as shown in Fig. 1(b). In this case, the transconductance behavior with various V_{BG} is not just threshold shift. The peak and the slope of transconductance may change due to the combination of the front and back mobilities, depending on the interfacial qualities of the front and back sides. This “anomalous” transconductance behavior can be observed when: 1) applying high V_{BG} [positive (negative) for n(p)MOSFET] to invert the back-side channel and 2) the front- (back)- gate oxide is thick (thin). Sentaurus technology computer-aided design (TCAD), which includes the density gradient quantization model and thin-layer mobility model with Philips unified mobility model [17], [18], is performed for the charge distribution. As shown in Fig. 1(c), a high V_{BG} leads to the back-side inversion, so the total current is affected by the front and back mobilities. Furthermore, the potential in the channel is determined by the front- and back-gate capacitances. A thick front-gate oxide would lead to less charges in the front channel and thus higher impact of the back-side charges and mobility. Therefore, both considering the front and back mobilities are crucial for the FDSOI MOSFET with wide range of biases and various device structures.

The linear region currents of FDSOI pMOSFETs with thick- and thin-front-gate oxide devices fabricated by a commercial foundry are measured, as shown in Fig. 2. Note that the device dimensions and bias conditions are similar to that in [13]. These two devices show distinct transconductance behaviors as shown in Figs. 3 and 4. The peak of transconductance of the thick front-gate oxide device (Fig. 3) nonmonotonically shifts (to the right at low $|V_{\text{GS}}|$ and then to the left at high $|V_{\text{GS}}|$) with increasing back-gate bias voltage (denote as “anomalous” transconductance), while that of the thin front-gate oxide device (Fig. 4) exhibits a monotonic characteristic with the back-gate bias voltage (to the left). It is observed that the single mobility model (dashed lines in Fig. 3) cannot capture the nonmonotonic shift of the transconductance peak. The transconductance peak is directly related to the turn-on

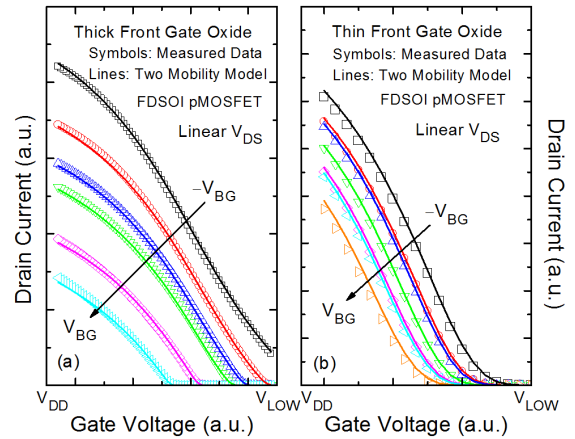


Fig. 2. $I_{\text{DS}}-V_{\text{GS}}$ curves of FDSOI pMOSFETs with (a) thick and (b) thin front-gate oxides at linear drain bias region. The same BOX and body thicknesses are used in both devices. The back-gate bias is applied from negative to positive.

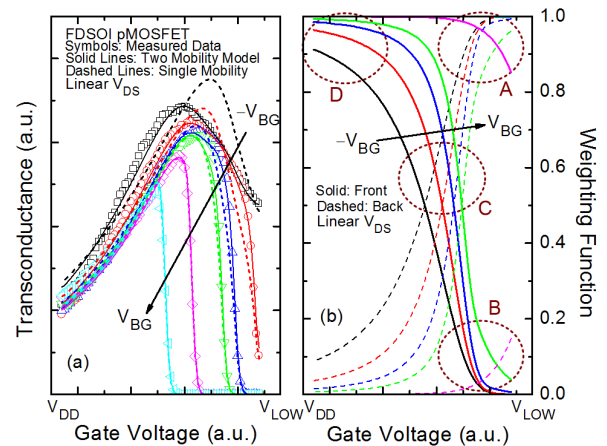


Fig. 3. (a) Transconductance and (b) extracted weighting function of an FDSOI pMOSFET with thick front-gate oxide at linear drain bias region. The back-gate bias is applied from negative to positive.

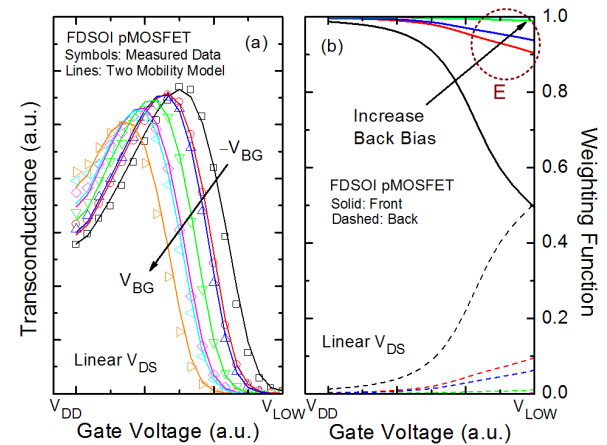


Fig. 4. (a) Transconductance and (b) extracted weighting function of an FDSOI pMOSFET with thin front-gate oxide at linear drain bias region. The back-gate bias is applied from negative to positive.

phenomenon of the multiple channels as well as the mobility [10] and a new model is required to capture this nonmonotonic effect.

$$\mu_{\text{eff}1(2)} = \frac{\mu_{1(2)}}{1 + (\text{UA}1(2) + \text{UC}1(2) \cdot V_{\text{BG}}) E_{\text{eff}1(2)}^{\text{EU}1(2)+\text{EUB}1(2) \cdot V_{\text{BG}}} + \frac{\text{UD}1(2)+\text{UDB}1(2) \cdot V_{\text{BG}}}{(0.5+0.5q_{\text{ia}}C_{\text{ox}})^{\text{UCS}1(2)}}} \quad (1)$$

B. Compact Modeling

Due to the back-gate bias, the charge centroid moves, resulting in back bias-dependent degradation and ambiguous effective electric field [8]. Furthermore, the back-side inversion or back-channel also affects the current and its derivative. That is, the device with thicker front-gate oxide sees more influence of the back gate in its behavior due to the weaker front-gate control. For this device, the front- and back-side channels co-exist and show different effective mobilities due to distinct qualities of front and back interfaces [9]. Moreover, the inversion charges of the front and back sides experience different electric fields because of the various applied biases scenario. According to above reasons, the mobility model based only on the front surface electrostatics may not be sufficient and a two-mobility model is required. For planar MOSFETs and FinFETs, the mobility model, which includes the surface roughness scattering and Coulombic scattering, has been widely used and is accurate [19], [20]. Thus, the mobility formulas for front- and back-side channels of FDSOI MOSFETs are similar but the parameters are separated. In (1), as shown at the top of this page, $\mu_{1(2)}$ is the low-field carrier mobility, $\text{UA}1(2)$, $\text{UC}1(2)$, $\text{EU}1(2)$, $\text{EUB}1(2)$, $\text{UD}1(2)$, $\text{UDB}1(2)$, and $\text{UCS}1(2)$ are the model parameters extracted from the experimental data, q_{ia} is the average charge in the channel in unit of volt, and $E_{\text{eff}1(2)}$ is the effective electric field [21]

$$E_{\text{eff}1(2)} = \frac{Q_{\text{dep}} + \eta Q_{\text{inv}1(2)}}{\epsilon_{\text{Si}}}$$

where Q_{dep} and $Q_{\text{inv}1(2)}$ are the depletion and inversion charges, ϵ_{Si} is the permittivity of silicon, and η is 1/2 for nMOSFET and 1/3 for pMOSFET. The parameters for the front- and back-side channels are denoted by “1” and “2,” respectively. The second term in the denominator of (1) represents the surface roughness scattering, and the third term stands for the Coulombic scattering [21]–[23].

The total effective mobility is calculated considering the front- and back-side mobilities in a weighted manner as [24]–[26]

$$\mu_{\text{total}} = w \cdot \mu_{\text{eff}1} + (1 - w) \cdot \mu_{\text{eff}2}. \quad (2)$$

The weights w in (2) is a dimensionless function of the ratio of charges. The more the amount of charge at an interface, the larger contribution in the effective mobility that interface makes, as shown in Fig. 3(b). The weighting functions in [24] are only valid for the strong inversion, and they are improved in this paper to capture both subthreshold and inversion regions. The amount of inversion charges is an exponential function of surface potential [27] derived from Poisson’s equation assuming Boltzmann statistics (approximation of Fermi–Dirac statistics). In the subthreshold region, the surface potential varies linearly with the gate bias, so the

inversion charge is an exponential function of the gate voltage. In the strong inversion, since the surface potential has weak dependence on the gate bias, the inversion charge shows linear dependence on the gate voltage [28]. Hence, the weighting functions for the front and back sides are

$$w = \frac{e^{(\phi_f - V_{\text{ch}})/V_t}}{e^{(\phi_f - V_{\text{ch}})/V_t} + e^{(\phi_b - V_{\text{ch}})/V_t}} = \frac{e^{\phi_f/V_t}}{e^{\phi_f/V_t} + e^{\phi_b/V_t}} \quad (3)$$

$$1 - w = \frac{e^{(\phi_b - V_{\text{ch}})/V_t}}{e^{(\phi_f - V_{\text{ch}})/V_t} + e^{(\phi_b - V_{\text{ch}})/V_t}} = \frac{e^{\phi_b/V_t}}{e^{\phi_f/V_t} + e^{\phi_b/V_t}} \quad (4)$$

where ϕ_f and ϕ_b are the surface potentials of the front and back channels, V_{ch} is the quasi-Fermi potential, and $V_t (= k_B T/q)$ is the thermal voltage. A thin front (back) gate oxide increases the surface potential of the front (back) channel, leading to higher weighting factors. If the front-gate oxide is thick enough (about one fifth of the back oxide), the back channel would be apparent in the g_m due to large weighting factor of the back-side as shown in Fig. 3(b). Finally, the total effective mobility is used into the drain current model [4], [27], [29].

C. Parameter Extraction Methodology

To evaluate the proposed model, the model parameters in (1) should be properly extracted. The general guideline of parameters extraction is shown in [22]. After extracting the model parameters for charges, threshold voltage, and subthreshold slope from the device $I_{\text{DS}}-V_{\text{GS}}$ plot, the mobility model parameters at strong inversion bias regime are then extracted as follows. First, the mobility parameters such as EU, UA, UD, and UCS for the front side are extracted for $V_{\text{BG}} = 0$. At $V_{\text{BG}} = 0$, these parameters do not depend on the back-gate bias. Then, only the back-gate bias-related parameters such as UC, EUB, and UDB for the front side at the back-side accumulation bias condition [negative (positive) V_{BG} for n(p)MOSFET] are extracted. Finally, all the parameters related to the back-side mobility are tuned at the back-side inversion bias condition [large positive (negative) V_{BG} for n(p)MOSFET].

III. RESULTS AND DISCUSSION

The two-mobility model has been incorporated into BSIM-IMG models. Fig. 5 shows the comparison of the model and the TCAD simulation data from [30] of the front-gate capacitances with the buried oxide (BOX) thicknesses of 10 and 20 nm. The core model described in [27] accurately captures the back-side inversion effect, which causes the first plateau of the gate capacitance at $V_{\text{BG}} = 3$ V. Based on the accurate charge and surface potential calculations from the core model, weighting functions (3) and (4) are robust. Fig. 2 shows that the proposed model matches well the experimental data of both thick and thin front-gate oxides FDSOI pMOSFETs. Fig. 3 shows the transconductance and

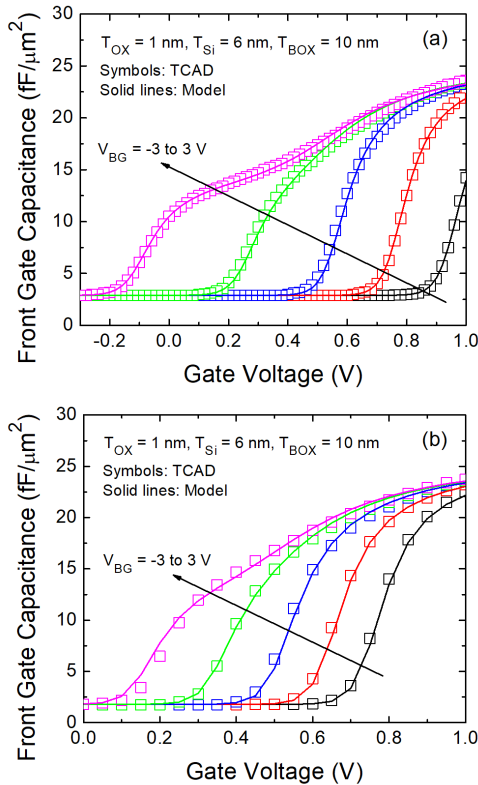


Fig. 5. The TCAD simulated front-gate capacitances [30] with the BOX thicknesses of (a) 10 and (b) 20 nm. The core model described in [27] for the charges and surface potentials accurately captures the back-side inversion effect.

extracted weighting function from experimental data for an FDSOI pMOSFET with thick front-gate oxide. At high $|V_{BG}|$ and low $|V_{GS}|$ (subthreshold region), i.e., the bias condition in which the back-side inversion occurs, the channel charge (hole) is dominated by the back-side channel charges and the weighting function of the back side is larger than that of the front side, as shown by circles A and B in Fig. 3(b). As the front-gate voltage increases, the weighting factor for the front side increases and the two factors cross, as shown by circle C in Fig. 3(b). Ultimately, the front weighting factor becomes much larger than the back one, indicating the domination of the front charge and mobility, as shown by circle D in Fig. 3(b). The crossing point happens near the onset of the surface roughness scattering. In other words, the front-channel charge concentration is high enough and the front-gate voltage attracts the inversion holes to the body/oxide interface, leading to scattering. For a thin front-gate oxide devices shown in Fig. 4, a different behavior of weighting function is found. The transconductance shows monotonic behavior with the back-gate bias, just like threshold voltage shift. This is due to the larger front-gate capacitance and charge in thin front-gate oxide device. Even at high $|V_{BG}|$, the front-channel charge dominates the effective mobility for this device, as shown by circle E in Fig. 4(b). It is worth noting that the different device behavior due to the front-gate oxide thickness change is captured physically in our model.

Fig. 6 shows the extracted effective mobility of the front and back channels as functions of the back-gate bias. The back-channel mobility always exceeds the front-channel mobility [9]

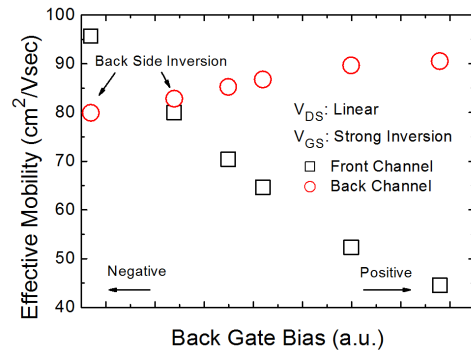


Fig. 6. Extracted effective mobility of the front and back channels from Fig. 2. The back-side inversion occurs when the back-gate bias is negative in FDSOI pMOSFET.

except at high $|V_{BG}|$. In addition, the dependence of the front-channel mobility on V_{BG} is opposite to that of the back-channel mobility, i.e., opposite sign of slope of mobility– V_{BG} plot. This is because more $|V_{BG}|$ attracts the front-channel holes toward the body but moves the back-channel holes closer to body/BOX interface, resulting in reduction of scattering for the front side but mobility degradation for the back-side. This effect is captured by model parameters UC and EUB. Furthermore, the front and back mobilities in Fig. 6 show different magnitude of slopes, indicating that the interfacial quality of the front and back surfaces is different for the surface roughness scattering [9]. In Fig. 7, the scalability of the BSIM-IMG model is demonstrated with another longer channel FDSOI pMOSFET with thick front-gate oxide using similar mobility parameters as the shorter channel device in Fig. 3. The nonmonotonic V_{BG} -dependence on the transconductance at the linear drain bias is observed [see Fig. 7(a) and (b)], indicating that the impact of the longitudinal electric field is less crucial to the mobility than the transverse one. The mobility is mainly influenced by the electric field from the front-gate and the back-gate. Moreover, the transconductance at the saturation drain bias is also accurately captured by the proposed model [see Fig. 7(c) and (d)], showing the model capability for the pinch off and the channel length modulation effects.

To examine the model for a different doping polarity, a long-channel FDSOI nMOSFET with the thick front-gate oxide is well fit with the developed model as shown in Fig. 8. Due to the smaller effective mass of electron, the charge centroid is closer to the back surface and thus the surface roughness scattering becomes more significant than that of hole [31]. Hence, the peak of transconductance of FDSOI nMOSFET with the thick front-gate oxide at the back-side inversion bias is not as apparent as FDSOI pMOSFET, as shown in Fig. 8(b). Fig. 9 shows measured data from the Laboratoire d'électronique et de technologie de l'information (LETI) device [21] and model results of an FDSOI nMOSFET. Different technologies from the other previously shown devices are adopted in Fig. 9, indicating that the proposed model is not only physical but also flexible for the technology variation. To further validate the developed model for the device

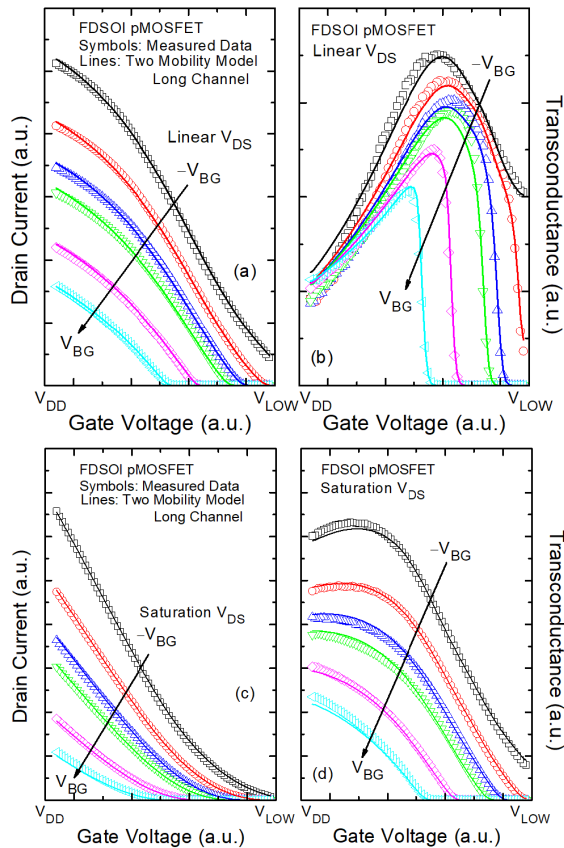


Fig. 7. I_{DS} - V_{GS} at (a) linear and (c) saturation drain biases, and transconductance at (b) linear and (d) saturation drain biases of a long-channel FDSOI pMOSFET with the same body and BOX thicknesses as the device shown in Fig. 3.

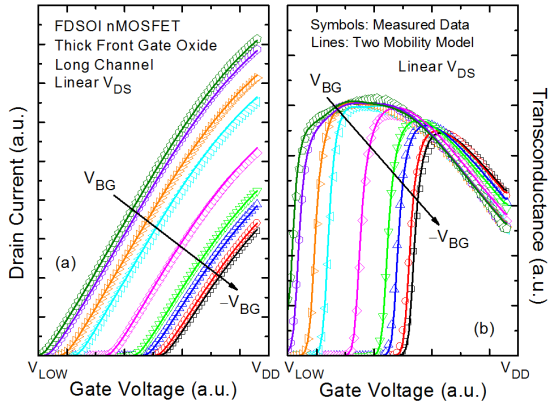


Fig. 8. (a) I_{DS} - V_{GS} and (b) transconductance of a long-channel FDSOI nMOSFET with thick front-gate oxide and similar device structure as the pMOSFET shown in Fig. 7.

scaling, a short-channel ($L = 20$ nm) FDSOI nMOSFET with $T_{BODY} = 4$ nm is simulated using Sentaurus TCAD with the density gradient quantization model and thin-layer mobility model with the Philips unified mobility model [17], [18], as shown in Fig. 10. The proposed model is in good agreement with the simulated data, showing great model capability of device scaling with even thinner body where the charge ratio of front and back sides are correctly captured by the core model.

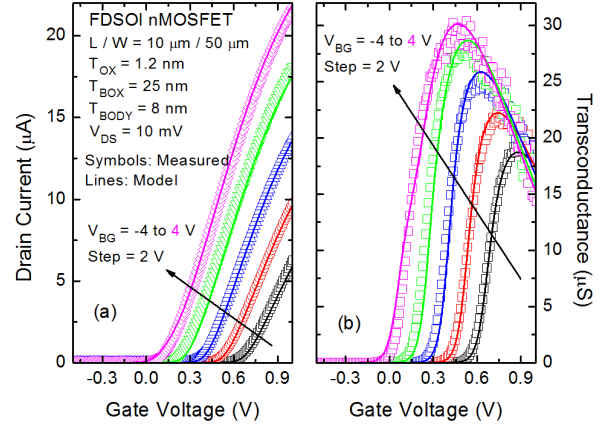


Fig. 9. (a) I_{DS} - V_{GS} and (b) transconductance of an FDSOI nMOSFET with $L = 10 \mu m$, $W = 50 \mu m$, $T_{OX} = 1.2$ nm, $T_{BOX} = 25$ nm, and $T_{BODY} = 8$ nm. Measurement data are from the LETI device [21].

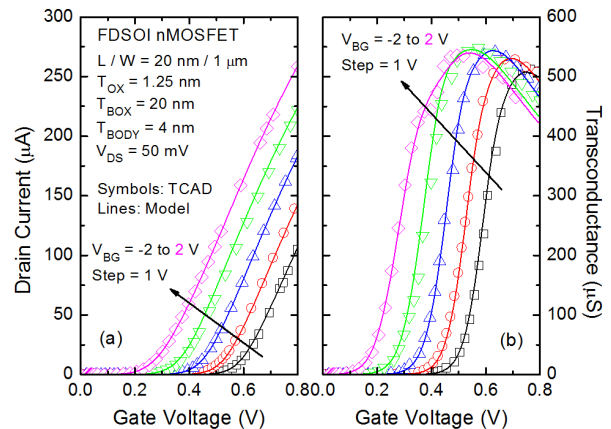


Fig. 10. TCAD simulated (a) I_{DS} - V_{GS} and (b) transconductance of an FDSOI nMOSFET with $L = 20$ nm, $W = 1 \mu m$, $T_{OX} = 1.25$ nm, $T_{BOX} = 20$ nm, and $T_{BODY} = 4$ nm at various V_{BG} .

IV. CONCLUSION

An anomalous transconductance in an FDSOI MOSFET with thick front-gate oxide is analyzed and modeled. By comparing devices with thin and thick front-gate oxides, it is found that the mobility in the back channel plays an important role in the nonmonotonic V_{BG} dependence. The total effective mobility is separated into two parts: front and back channels, weighted by charge-based factors. The proposed model is implemented into BSIM-IMG and is validated against the experimental and TCAD simulated data for multiple FDSOI devices, which would benefit circuit applications such as image sensors and high-voltage devices.

REFERENCES

- [1] K. Uchida, J. Koga, R. Ohba, T. Numata, and S. I. Takagi, "Experimental evidences of quantum-mechanical effects on low-field mobility, gate-channel capacitance, and threshold voltage of ultrathin body SOI MOSFETs," in *IEDM Tech. Dig.*, Dec. 2001, pp. 29.4.1–29.4.4, doi: [10.1109/IEDM.2001.979588](https://doi.org/10.1109/IEDM.2001.979588).
- [2] D. Ha, H. Takeuchi, Y.-K. Choi, and T.-J. King, "Molybdenum gate technology for ultrathin-body MOSFETs and FinFETs," *IEEE Trans. Electron Devices*, vol. 51, no. 12, pp. 1989–1996, Dec. 2004, doi: [10.1109/TED.2004.839752](https://doi.org/10.1109/TED.2004.839752).

- [3] O. Faynot *et al.*, "Planar fully depleted SOI technology: A powerful architecture for the 20 nm node and beyond," in *IEDM Tech. Dig.*, Dec. 2011, pp. 3.2.1–3.2.4, doi: [10.1109/IEDM.2010.5703287](https://doi.org/10.1109/IEDM.2010.5703287).
- [4] S. Khandelwal *et al.*, "BSIM-IMG: A compact model for ultrathin-body SOI MOSFETs with back-gate control," *IEEE Trans. Electron Devices*, vol. 59, no. 8, pp. 2019–2026, Aug. 2012, doi: [10.1109/TED.2012.2198065](https://doi.org/10.1109/TED.2012.2198065).
- [5] Y.-K. Lin *et al.*, "Modeling of back-gate effects on gate-induced drain leakage and gate currents in UTB SOI MOSFETs," *IEEE Trans. Electron Devices*, vol. 64, no. 10, pp. 3986–3990, Oct. 2017, doi: [10.1109/TED.2017.2735455](https://doi.org/10.1109/TED.2017.2735455).
- [6] A. Ohata, S. Cristoloveanu, and M. Casse, "Mobility comparison between front and back channels in ultrathin silicon-on-insulator metal-oxide-semiconductor field-effect transistors by the front-gate split capacitance-voltage method," *Appl. Phys. Lett.*, vol. 89, no. 3, pp. 032104-1–032104-3, Jul. 2006, doi: [10.1063/1.2222255](https://doi.org/10.1063/1.2222255).
- [7] S. Cristoloveanu, N. Rodriguez, and F. Gamiz, "Why the universal mobility is not," *IEEE Trans. Electron Devices*, vol. 57, no. 6, pp. 1327–1333, Jun. 2010, doi: [10.1109/TED.2010.2046109](https://doi.org/10.1109/TED.2010.2046109).
- [8] C. Navarro *et al.*, "Multibranch mobility analysis for the characterization of FDSOI transistors," *IEEE Electron Device Lett.*, vol. 33, no. 8, pp. 1102–1104, Aug. 2012, doi: [10.1109/LED.2012.2198193](https://doi.org/10.1109/LED.2012.2198193).
- [9] T. Rudenko *et al.*, "Experimental study of transconductance and mobility behaviors in ultra-thin SOI MOSFETs with standard and thin buried oxides," *Solid-State Electron.*, vol. 54, no. 2, pp. 164–170, Feb. 2010, doi: [10.1016/j.sse.2009.12.014](https://doi.org/10.1016/j.sse.2009.12.014).
- [10] H. Agarwal, C. Gupta, S. Dey, S. Khandelwal, C. Hu, and Y. S. Chauhan, "Anomalous transconductance in long channel halo implanted MOSFETs: Analysis and modeling," *IEEE Trans. Electron Devices*, vol. 64, no. 2, pp. 376–383, Feb. 2017, doi: [10.1109/TED.2016.2640279](https://doi.org/10.1109/TED.2016.2640279).
- [11] C. Fenouillet-Beranger *et al.*, "Efficient multi-VT FDSOI technology with UTBOX for low power circuit design," in *VLSI Symp. Tech. Dig.*, Jun. 2010, pp. 65–66, doi: [10.1109/VLSIT.2010.5556118](https://doi.org/10.1109/VLSIT.2010.5556118).
- [12] A. Litty, S. Ortolland, D. Golanski, and S. Cristoloveanu, "Dual ground plane EDMOS in ultrathin FDSOI for 5V energy management applications," in *Proc. 44th Eur. Solid State Device Res. Conf. (ESSDERC)*, Sep. 2014, pp. 134–137, doi: [10.1109/ESSDERC.2014.6948776](https://doi.org/10.1109/ESSDERC.2014.6948776).
- [13] V. Suntharalingam *et al.*, "Megapixel CMOS image sensor fabricated in three-dimensional integrated circuit technology," in *IEEE Int. Solid-State Circuits Conf. (ISSCC) Dig. Tech. Papers*, Feb. 2005, pp. 356–357, doi: [10.1109/ISSCC.2005.1494016](https://doi.org/10.1109/ISSCC.2005.1494016).
- [14] M. Goto *et al.*, "Pixel-parallel 3-D integrated CMOS image sensors with pulse frequency modulation A/D converters developed by direct bonding of SOI layers," *IEEE Trans. Electron Devices*, vol. 62, no. 11, pp. 3530–3535, Nov. 2015, doi: [10.1109/TED.2015.2425393](https://doi.org/10.1109/TED.2015.2425393).
- [15] P. Coudrain *et al.*, "Investigation of a sequential three-dimensional process for back-illuminated CMOS image sensors with miniaturized pixels," *IEEE Trans. Electron Devices*, vol. 56, no. 11, pp. 2403–2413, Nov. 2009, doi: [10.1109/TED.2009.2030990](https://doi.org/10.1109/TED.2009.2030990).
- [16] E. R. Fossum, "CMOS image sensors: Electronic camera-on-a-chip," *IEEE Trans. Electron Devices*, vol. 44, no. 10, pp. 1689–1698, Oct. 1997, doi: [10.1109/16.628824](https://doi.org/10.1109/16.628824).
- [17] *Sentaurus Device User Guide, Version M-2016.12*, Synopsys, Mountain View, CA, USA, Dec. 2016.
- [18] S. Reggiani, E. Gnani, A. Gnudi, M. Rudan, and G. Bacarani, "Low-field electron mobility model for ultrathin-body SOI and double-gate MOSFETs with extremely small silicon thicknesses," *IEEE Trans. Electron Devices*, vol. 54, no. 9, pp. 2204–2212, Sep. 2007, doi: [10.1109/TED.2007.902899](https://doi.org/10.1109/TED.2007.902899).
- [19] Y. S. Chauhan *et al.*, "BSIM6: Analog and RF compact model for bulk MOSFET," *IEEE Trans. Electron Devices*, vol. 61, no. 2, pp. 234–244, Feb. 2014, doi: [10.1109/TED.2013.2283084](https://doi.org/10.1109/TED.2013.2283084).
- [20] Y. S. Chauhan, *FinFET Modeling for IC Simulation and Design: Using the BSIM-CMG Standard*. San Diego, CA, USA: Academic, 2015.
- [21] P. Kushwaha *et al.*, "Predictive effective mobility model for FDSOI Transistors using technology parameters," in *Proc. IEEE Int. Conf. Electron Devices Solid-State Circuits (EDSSC)*, Aug. 2016, pp. 448–451, doi: [10.1109/EDSSC.2016.7785304](https://doi.org/10.1109/EDSSC.2016.7785304).
- [22] *BSIM-IMG102.8.0 Technical Manual*. Accessed: Nov. 30, 2016. [Online]. Available: <http://bsim.berkeley.edu/models/bsimimg/>
- [23] S. Khandelwal, J. P. Duarte, Y. S. Chauhan, and C. Hu, "Modeling 20-nm germanium FinFET with the industry standard FinFET model," *IEEE Electron Device Lett.*, vol. 35, no. 7, pp. 711–713, Jul. 2014, doi: [10.1109/LED.2014.2323956](https://doi.org/10.1109/LED.2014.2323956).
- [24] Y. Sahu, P. Kushwaha, A. Dasgupta, C. Hu, and Y. S. Chauhan, "Compact modeling of drain current thermal noise in FDSOI MOSFETs including back-bias effect," *IEEE Trans. Microw. Theory Techn.*, vol. 65, no. 7, pp. 2261–2270, Jul. 2017, doi: [10.1109/TMTT.2017.2666811](https://doi.org/10.1109/TMTT.2017.2666811).
- [25] T. Poiroux *et al.*, "Leti-UTSOI2.1: A compact model for UTBB-FDSOI technologies—Part I: Interface potentials analytical model," *IEEE Trans. Electron Devices*, vol. 62, no. 9, pp. 2751–2759, Sep. 2015, doi: [10.1109/TED.2015.2458339](https://doi.org/10.1109/TED.2015.2458339).
- [26] T. Poiroux *et al.*, "Leti-UTSOI2.1: A compact model for UTBB-FDSOI technologies—Part II: DC and AC model description," *IEEE Trans. Electron Devices*, vol. 62, no. 9, pp. 2760–2768, Sep. 2015, doi: [10.1109/TED.2015.2458336](https://doi.org/10.1109/TED.2015.2458336).
- [27] J. P. Duarte *et al.*, "Modeling independent multi-gate MOSFET," in *Proc. Workshop Compact Modeling (WCM)*, May 2016, pp. 1–6.
- [28] Y. Tsididis and C. McAndrew, *Operation and Modeling of the MOS Transistor*, 3rd ed. New York, NY, USA: Oxford Univ. Press, 2011.
- [29] A. Ortiz-Conde and F. J. G. Sánchez, "Unification of asymmetric DG, symmetric DG and bulk undoped-body MOSFET drain current," *Solid-State Electron.*, vol. 50, nos. 11–12, pp. 1796–1800, Nov./Dec. 2006, doi: [10.1016/j.sse.2006.10.003](https://doi.org/10.1016/j.sse.2006.10.003).
- [30] T. Poiroux *et al.*, "UTSOI2: A complete physical compact model for UTBB and independent double gate MOSFETs," in *IEDM Tech. Dig.*, Dec. 2013, pp. 12.4.1–12.4.4, doi: [10.1109/IEDM.2013.6724616](https://doi.org/10.1109/IEDM.2013.6724616).
- [31] S. Takagi, M. Takayanagi, and A. Toriumi, "Characterization of inversion-layer capacitance of holes in Si MOSFETs," *IEEE Trans. Electron Devices*, vol. 46, no. 7, pp. 1446–1450, Jul. 1999.



Yen-Kai Lin (S'15) received the B.S. degree in physics and the M.S. degree in electronics engineering from National Taiwan University, Taipei, Taiwan, in 2013 and 2014, respectively. He is currently pursuing the Ph.D. degree in electrical engineering with the University of California, Berkeley, CA, USA.

Since 2015, he has been with the BSIM Group, Berkeley, CA, USA. His current research interests include compact modeling and simulation of advanced devices.

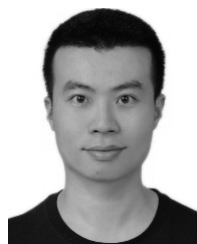


Pragya Kushwaha received the Ph.D. degree from the Department of Electrical Engineering, IIT Kanpur, Kanpur, India.

She was a Co-Developer of the BSIM compact models with the BSIM Group, University of California, Berkeley, CA, USA, where she is currently a Post-Doctoral Researcher. Her current research interests include modeling, simulation, and characterization of semiconductor devices such as nanowires, NCFETs, PD/FDSOIs, FinFETs, tunnel FETs, high-voltage FETs, and bulk MOSFETs.



Juan Pablo Duarte (S'12) received the B.S. and M.S. degrees in electrical engineering, from the Korea Advanced Institute of Science and Technology, Daejeon, South Korea, in 2010 and 2012, respectively, and the Ph.D. degree in electrical engineering from the University of California, Berkeley, CA, USA, in 2017.



Huan-Lin Chang (S'07–M'11) received the Ph.D. degree in electronics engineering from National Taiwan University, Taipei, Taiwan, in 2011.

He was with SPICE Team, Taiwan Semiconductor Manufacturing Company, from 2011 to 2015. Then, he joined the BSIM Group as a Post-Doctoral Researcher with University of California, Berkeley, CA, USA. His current research interests include compact modeling of the semiconductor devices.



Harshit Agarwal received the Ph.D. degree from IIT Kanpur, Kanpur, India.

He is currently a Post-Doctoral Researcher/Manager with the Device Modeling Center, BSIM Group, UC Berkeley, Berkeley, CA, USA. His current research interests include the modeling and characterization of high-voltage devices, NCFETs, FinFETs, and GAA FETs.



Yogesh Singh Chauhan (SM'12) is currently an Associate Professor with the Department of Electrical Engineering, IIT Kanpur, Kanpur, India. He is the Lead Developer of industry standard BSIM-BULK model and a Co-Developer of ASM-HEMT model for GaN HEMTs, which is under industry standardization at the Compact Model Coalition, Austin, TX, USA. His current research interests include characterization, modeling, and simulation of semiconductor devices.



Sourabh Khandelwal (M'14) was as Research Engineer with IBM Semiconductor Research, New Delhi, India. He was the Manager and Post-Doctoral Researcher with the Berkeley Device Modeling Center, BSIM Group, University of California at Berkeley, Berkeley, CA, USA. He is currently an Assistant Professor with the School of Science and Engineering, Macquarie University, Sydney, NSW, Australia. He is the Lead Developer of ASM-GaN-HEMT compact model for the emerging GaN technology with Compact Model Coalition, Austin, TX, USA.



Sayeef Salahuddin (SM'14) received the B.Sc. degree in electrical and electronic engineering from the Bangladesh University of Engineering and Technology, Dhaka, Bangladesh, in 2003, and the Ph.D. degree in electrical and computer engineering from Purdue University, West Lafayette, IN, USA, in 2007.

He joined the Faculty of Electrical Engineering and Computer Science, University of California, Berkeley, CA, USA, in 2008.



Angada B. Sachid (M'11) received the Ph.D. degree in electrical engineering from IIT Bombay, Mumbai, India, in 2010.

He is currently a Post-Doctoral Researcher with Electrical Engineering and Computer Sciences, University of California at Berkeley, Berkeley, CA, USA.



Chenming Hu (LF'16) is currently a Distinguished Professor Emeritus with the University of California, Berkeley, CA, USA. He is also a Board Director of SanDisk Inc., Milpitas, CA, USA, and Friends of Children with Special Needs, Fremont, CA, USA. He is known for his work on FinFET—the 3-D transistor, widely used IC reliability models, and BSIM—the industry standard transistor models used by most IC companies since 1997 to design CMOS products.

Michael Harter, photograph and biography not available at the time of publication.

Josef Watts, photograph and biography not available at the time of publication.